Spontaneous bending of 2D molecular bottle-brush

Subbotin, A; Jong, J; ten Brinke, G

Published in:
European Physical Journal E

DOI:
10.1140/epje/i2005-10122-7

Publication date:
2006

Eur. Phys. J. E **20**, 99–108 (2006)
DOI 10.1140/epje/i2005-10122-7

THE EUROPEAN PHYSICAL JOURNAL E

Spontaneous bending of 2D molecular bottle-brush

A. Subbotin[1,2,a], J. de Jong[2], and G. ten Brinke[2,b]

[1] Institute of Petrochemical Synthesis, Russian Academy of Sciences, Moscow 119991, Russia
[2] Laboratory of Polymer Chemistry and Materials Science Centre, University of Groningen, Nijenborgh 4, 9747 AG Groningen, The Netherlands

Received 15 December 2005 and Received in final form 15 March 2006 /
Published online: 15 May 2006 –

Abstract. Using a scaling approach we consider a 2D comb copolymer brush under bending deformations. We show that the rectilinear brush is locally stable and can be characterized by a persistence length λ increasing with the molecular weight of grafting side chains as $\lambda \sim M^3$. A bending instability due to redistribution of the side chains appears in the non-linear regime where bending is strong. Arguments are presented that the brush conformations consist of alternating rectilinear and bent sections corresponding to the different free-energy minima.

PACS. 82.35.Jk Copolymers, phase transitions, structure – 89.75.Fb Structures and organization in complex systems

1 Introduction

Comb copolymer brushes with high grafting density (bottle-brushes) have been extensively studied during the last decades, theoretically [1–5], experimentally [6–9] and using computer simulations [10–14]. Theoretical calculations based on scaling [2] and mean-field [3] approaches show that the steric repulsion between the flexible side chains induces bending rigidity for 3D cylindrical brushes when the molecular weight of the side chains increases. This effect was also recently confirmed by means of a more accurate self-consistent field approach [5]. The numerical calculations demonstrated that some discrepancy between the theory and computer simulations for moderate chain lengths can be explained by the very small numerical prefactor in the dependencies between the persistence length and side chain molecular weight.

Another situation occurs for bottle-brushes with chemically different side chains. Due to incompatibility between the different chain species and their corresponding redistribution the bottle-brush can spontaneously bend. This effect was predicted for 3D brushes theoretically [4] and confirmed with computer simulation studies [14]. For adsorbed brushes with chemically different side chains (2D case) bent conformations were found experimentally [9]. Spontaneous bending also appears in the 2D case when chemically identical side chains are distributed non- symmetrically with respect to the backbone [15]. All of these effects are physically clear and are connected with the broken symmetry of the brush.

Recently Potemkin and coworkers predicted that rectilinear 2D molecular bottle-brushes exhibit a bending instability even under small fluctuations when chemically identical side chains are free to redistribute with respect to the backbone [16,17]. This result was obtained using a mean-field approach with the Alexander-de Gennes approximation for the position of the free chain ends. The presence of a bending instability was also confirmed experimentally [17,18] and with computer simulations [19].

It is well known, however, that in equilibrium the free ends of a rectilinear bottle-brush are distributed throughout the whole layer. The case where the free ends are all located at the same distance from the backbone does not correspond to the minimum of the free energy and, therefore, corresponds to a non- equilibrium situation. It implies that the local bending instability of the rectilinear 2D brush predicted may be a real physical effect or alternatively may be simply due to the use of the non-equilibrium rectilinear brush conformation. In this paper we address this question. Using mean-field calculations with relaxing free ends we demonstrate in Appendices A and B that allowance for a free-end distribution implies that the rectilinear conformation of the 2D brush is locally stable. In the main body of this paper we show that the same result is found using a simple 2D blob model [20]. This approach is

[a] e-mail: subbotin@ips.ac.ru
[b] e-mail: g.ten.brinke@rug.nl

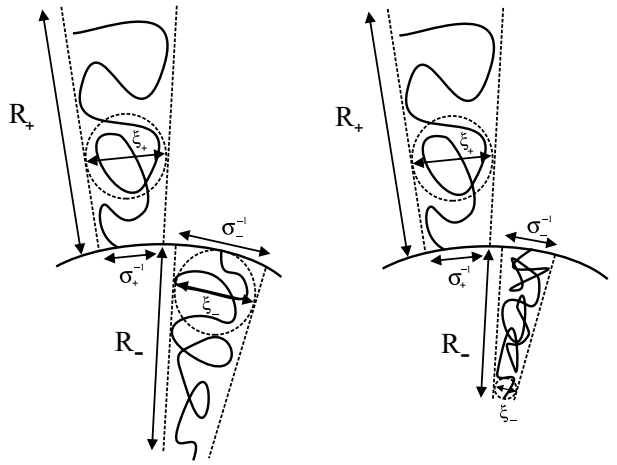

Fig. 1. Illustration of the blob picture for side chains for a bent backbone with constant curvature: (a) the Daoud-Cotton blob picture for both the convex and the concave part. This picture is realized in the weak-bending regime, (b) the Daoud-Cotton blob picture for the convex part and the semidilute-solution blob picture for the concave part. This picture corresponds to the strong-bending regime.

then used to demonstrate that a bending instability indeed appears but only in the non-linear deformation regime.

2 Stability analysis of the rectilinear conformation

We start with an infinitesimally small bending of the backbone, see Figure 1, and use the following notations: σ denotes the grafting density of side chains, $C = 1/R$ the curvature of the backbone (R is the radius of curvature) and M the number of segments per side chain. The free energy upon bending can be expanded with respect to C when the bending is small, *i.e.* $CR^* \ll C/\sigma \ll 1$, where R^* is the thickness of the side chain layer. It will be expressed as the sum of the free energy of the convex and concave part and the free energy of mixing for the side chain distribution. Let $\sigma_+ = \sigma^*(1+p)$, where $\sigma^* = \sigma/2$, denotes the grafting density of the convex part and similarly $\sigma_- = \sigma^*(1-p)$ for the concave part. Then, per unit backbone length the free-energy expansion can be written as

$$F = \mathcal{F}(\sigma_+) - \mathcal{H}(\sigma_+)C + \frac{1}{2}\mathcal{K}(\sigma_+)C^2 + \mathcal{F}(\sigma_-) + \mathcal{H}(\sigma_-)C + \frac{1}{2}\mathcal{K}(\sigma_-)C^2 + \sigma^*[(1+p)\ln(1+p) + (1-p)\ln(1-p)]. \quad (1)$$

Here $\mathcal{F}(\sigma)$, $\mathcal{H}(\sigma)$ and $\mathcal{K}(\sigma)$ are expansion parameters that are determined by the chain model used. For $p \ll 1$ the free energy can be expanded and minimized with respect to p. The mixing term does not contain any first-order contribution, therefore the free energy is expanded up to second order,

$$F = 2\mathcal{F}(\sigma^*) + \mathcal{F}''(\sigma^*){\sigma^*}^2p^2 - 2\mathcal{H}'(\sigma^*)\sigma^*pC + \left(\mathcal{K}(\sigma^*) + \frac{1}{2}\mathcal{K}''(\sigma^*){\sigma^*}^2p^2\right)C^2 + \sigma^*p^2. \quad (2)$$

Minimizing the free energy with respect to p gives

$$p = \frac{2\mathcal{H}'(\sigma^*)C}{2\mathcal{F}''(\sigma^*)\sigma^* + \mathcal{K}''(\sigma^*)\sigma^*C^2 + 2} \quad (3)$$

and thus for the free energy

$$F = 2\mathcal{F}(\sigma^*) + \left[\mathcal{K}(\sigma^*) - \frac{2\sigma^*{\mathcal{H}'}^2(\sigma^*)}{2 + 2\sigma^*\mathcal{F}''(\sigma^*) + \mathcal{K}''(\sigma^*)\sigma^*C^2}\right]C^2. \quad (4)$$

Hence, the change in free energy upon bending (C is small) can be written as

$$\Delta F = \left[\mathcal{K}(\sigma^*) - \frac{\sigma^*{\mathcal{H}'}^2(\sigma^*)}{1 + \sigma^*\mathcal{F}''(\sigma^*)}\right]C^2 = \frac{1}{2}\lambda C^2. \quad (5)$$

When the persistence length λ is negative, the free energy is lowered and there is an instability towards bending.

We will now use scaling arguments to calculate the expansion parameters. Consider the situation in Figure 1 (the convex layer). For the size of a blob at a distance x from the backbone the correlation length is given by

$$\xi_+(x) = \sigma_+^{-1}(1 + Cx) = am^\nu. \quad (6)$$

Here a is the statistical segment length, m is the number of segments per blob and ν is the scaling exponent (for self-avoiding walks in 2D $\nu = 3/4$). The density of segments satisfies

$$\rho_+(x) \simeq \frac{m}{\xi_+(x)^2} = \frac{1}{a^{1/\nu}}\sigma_+^{\frac{2\nu-1}{\nu}}(1 + Cx)^{\frac{1-2\nu}{\nu}}. \quad (7)$$

The free energy per blob equals kT, so for the 2D free-energy density we have

$$f_+(x) \simeq kT/\xi_+(x)^2. \quad (8)$$

The total number of segments per side chain M and the end-to-end point distance R_+ are related by

$$M = \frac{1}{\sigma_+}\int_0^{R_+} \mathrm{d}x(1 + Cx)\rho_+(x) \simeq \left(\frac{1}{a\sigma_+}\right)^{1/\nu}\frac{\nu\sigma_+}{C}\left[(1 + CR_+)^{1/\nu} - 1\right]. \quad (9)$$

Eliminating CR_+ from this equation and substituting its value into the free-energy expression gives (per unit

backbone length and in units of kT)

$$F_+ = \int_0^{R_+} \mathrm{d}x(1+Cx)f_+(x) \simeq \frac{\nu\sigma_+^2}{C}\ln\left[1+\frac{1}{\nu}MCa(\sigma_+ a)^{\frac{1-\nu}{\nu}}\right]$$
$$= \frac{M}{a}(\sigma_+ a)^{\frac{1+\nu}{\nu}} - \frac{M^2}{2\nu}(\sigma_+ a)^{\frac{2}{\nu}}C + \frac{M^3 a}{3\nu^2}(\sigma_+ a)^{\frac{3-\nu}{\nu}}C^2$$
$$= \mathcal{F}(\sigma_+) - \mathcal{H}(\sigma_+)C + \frac{1}{2}\mathcal{K}(\sigma_+)C^2. \quad (10)$$

Similarly we can write the free energy for the concave layer. Taking into account that the correlation length is given by $\xi_-(x) = \sigma_-^{-1}(1-Cx)$ the free energy is

$$F_- = \int_0^{R_-} \mathrm{d}x(1-Cx)f_-(x) \simeq$$
$$-\frac{\nu\sigma_-^2}{C}\ln\left[1-\frac{1}{\nu}MCa(\sigma_- a)^{\frac{1-\nu}{\nu}}\right]. \quad (11)$$

For the rectilinear brush $R_+ = R_- = R^* = Ma(\sigma^* a)^{1/3}$. After substitution of the expansion parameters in equation (5) we find that the 2D brush is stable, *i.e.* it does not curve spontaneously. This conclusion is in complete agreement with an alternative mean-field approach analysis using a free-ends distribution and which is presented in Appendices A and B. It is similar to the Birshtein and Zhulina [21] result on the stability of a plane bilayer with respect to cylindrical deformations. The persistence length of the straight brush having long side chains is approximately given by

$$\lambda \simeq \frac{2(2\nu-1)}{3\nu^2(1+\nu)}a\left(Ma\sigma^*\right)^3 = \frac{64}{189}a\left(Ma\sigma^*\right)^3. \quad (12)$$

3 Analysis of bent conformations

In this section we examine the free energy for strong bending. Based on the equations (10, 11) for the convex and concave layers we write the free energy per side chain as

$$F = \frac{1}{2\sigma^*}(F_+ + F_-)$$
$$\simeq \frac{3}{8}F^*\left[\frac{(1+p)^2}{CR^*}\ln\left[1+\frac{4}{3}CR^*(1+p)^{1/3}\right]\right.$$
$$\left.-\frac{(1-p)^2}{CR^*}\ln\left[1-\frac{4}{3}CR^*(1-p)^{1/3}\right]\right]. \quad (13)$$

Here $F^* = kTM(\sigma^* a)^{4/3}$ is the energy of the side chain for the rectilinear brush. In equation (13) we omitted the mixing entropy term as it is small. The results of the free-energy numerical minimization with respect to p for different values of curvature are shown in Figure 2, curve 1. The free energy passes through a maximum value and then decreases. The decreasing free-energy regime can be considered to correspond to spontaneous bending.

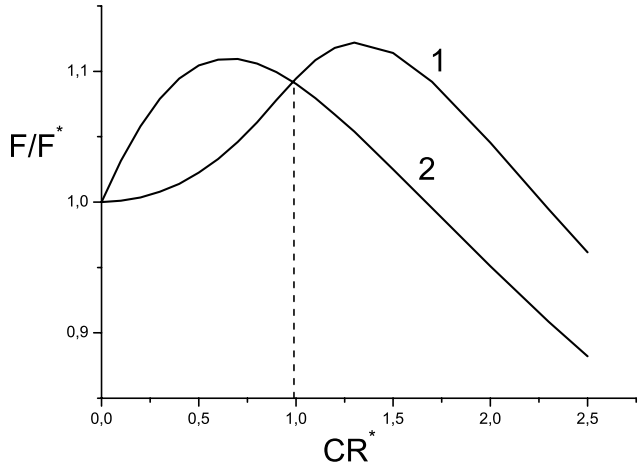

Fig. 2. The free energy as a function of curvature: curve 1 corresponds to the Daoud-Cotton blob picture for both convex and concave parts, and curve 2 corresponds to the Daoud-Cotton blob picture for the convex part and the semidilute-solution blob picture for the concave part (2).

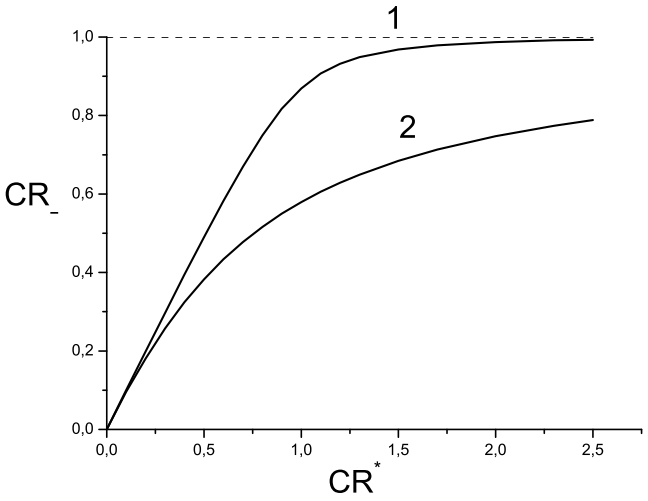

Fig. 3. Thickness of concave layer for the Daoud-Cotton blob picture (curve 1) and for the semidilute-solution blob picture (curve 2).

Note, however, that the assumption about the structure of the concave layer as a sequence of blobs with decreasing size leads to difficulties in the strong-bending regime as the different side chain trajectories start to cross each other at the focal point. Curve 1 of Figure 3 shows CR_- as a function of curvature as follows from the minimization of equation (13). When CR_- approaches 1, this blob picture is expected to break down and the concave layer will be more compressed. This observation suggests that in the case of strong bending it is more reasonable to assume a homogeneous distribution of segments (similar to a semidilute solution) inside the concave layer of thickness $R_- < C^{-1}$. The blob size ξ_- is then determined as the blob size on the boundary (see Fig. 1(b)) and, therefore, the correlation length inside the whole layer is given

by

$$\xi_- = \sigma_-^{-1}(1 - CR_-). \tag{14}$$

The surface area per grafting chain equals

$$S = \frac{R_-(2 - CR_-)}{2\sigma_-}.$$

Hence, the 2D concentration of segments is given by $\phi = M/S = (1/a^2)(a/\xi_-)^{2/3}$. This allows us to express the thickness R_- in terms of the parameter p as follows:

$$\frac{R_-(2 - CR_-)}{2(1 - CR_-)^{2/3}} = R^* (1 - p)^{1/3}. \tag{15}$$

The free energy of the concave layer is given by (per unit backbone length)

$$F_- \simeq \frac{\sigma_- S}{\xi_-^2} = \frac{\sigma_-^2 R_-(2 - CR_-)}{C(1 - CR_-)^2} \tag{16}$$

which leads to a total energy per side chain

$$F \simeq \frac{F^*}{2}\left[\frac{3}{4}\frac{(1+p)^2}{CR^*}\ln\left[1 + \frac{4}{3}CR^*(1+p)^{1/3}\right] + \frac{(1-p)^{7/3}}{CR^*(1 - CR_-)^{4/3}}\right]. \tag{17}$$

Numerical minimization of this with respect to p with the additional condition (15) gives the free energy as a function of curvature as plotted in Figure 2, curve 2. After a critical point ($CR^* \approx 1$, see Fig. 2) the non-homogeneous concave layer transforms into a homogeneous one. From there on the free energy always decreases with increasing curvature and has no minimum, a situation that can be described as spontaneous curvature. However, this spontaneous bending will be stabilized by excluded-volume interactions between distant parts of the brush. The thickness of the concave layer as a function of curvature as follows from the minimization of the free energy is shown by curve 2 in Figure 3. Generally we can also imagine the layer to consist of homogeneous and non-homogeneous parts (the intermediate case between the two limiting regimes considered above). However, calculations show that this situation does not occur. It implies that there is a sharp transition between the stable rectilinear regime and the unstable bending regime. The potential barrier (per side chain) for the transition to the spontaneous-bending regime according to the above picture is $\Delta F \simeq 0.09F^*$.

Now we take the stabilization effect into account and consider a bent brush consisting of two rectilinear sections connected by a bent section, see Figure 4. We will describe the shape of the bent backbone between the two rectilinear sections by the function $f(z)$. This function should be found from a free-energy minimization. In order to simplify the minimization procedure we select a trial function $f(z) = A\sin(qz)$ characterized by two parameters A and q. The curvature of the backbone is given by

$$C(z) = \frac{\mid f''(z) \mid}{(1 + f'^2(z))^{3/2}} = \frac{Aq^2 \sin qz}{(1 + (Aq)^2\cos^2 qz)^{3/2}}. \tag{18}$$

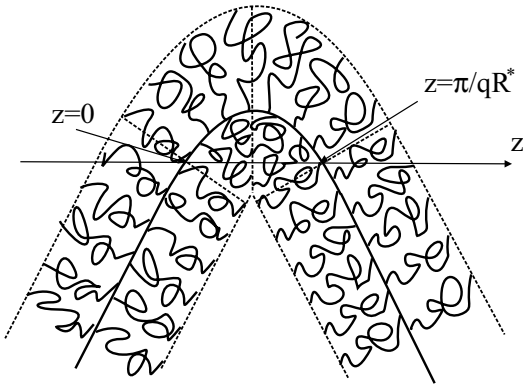

Fig. 4. Illustration of the strong-bending regime when the bending instability of the backbone is stabilized by the interaction between the distant side chains.

It is zero at the end points giving a smooth transition between the rectilinear and bent sections of the brush. Due to the non-homogeneous distribution of side chains along the backbone we should expect that the side chain trajectories will slightly deviate from the rectilinear one. However, we neglect this effect and assume that all trajectories are directed along the radius of curvature. For the convex layer we use the same blob picture as for the circularly shaped backbone. The only difference is that the grafting density now depends on z, $\sigma_+(z) = \sigma^*(1 + p(z))$. Taking into account that the length element of the backbone equals $\mathrm{d}l = \mathrm{d}z\sqrt{1 + f'^2(z)}$, the free energy per unit backbone length for the convex part is given by

$$F_+ \simeq \frac{\frac{3}{4}\int_0^{\frac{\pi}{2q}} \mathrm{d}z \frac{\sigma_+^2(z)\sqrt{1+f'^2(z)}}{C(z)} \ln\left[1 + \frac{4}{3}MC(z)a(\sigma_+(z)a)^{\frac{1}{3}}\right]}{\int_0^{\frac{\pi}{2q}} \mathrm{d}z\sqrt{1 + f'^2(z)}}. \tag{19}$$

For the concave layer we assume that the correlation length is fixed along the radius of curvature for each side chain, but it may change along the backbone. The length of the side chain trajectory is restricted by the symmetrical side chain from the second half of the backbone (see Fig. 4) and equals

$$R_- = \frac{(\pi/2 - qz)}{q}\frac{\sqrt{1 + f'^2(z)}}{f'(z)}. \tag{20}$$

Further, using the same arguments as for the homogeneous concave layer of the circularly shaped backbone we find for the energy of the concave layer (per unit backbone length)

$$F_- \simeq \frac{\int_0^{\frac{\pi}{2q}} \mathrm{d}z \frac{\sigma_-^2(z)\left(1+f'^2(z)\right)\left(\frac{\pi}{2} - qz\right)}{2qf'(z)} \frac{(2qf'(z)\left(1+f'^2(z)\right) - \left(\frac{\pi}{2} - qz\right)|f''(z)|)}{(qf'(z)(1+f'^2(z)) - \left(\frac{\pi}{2} - qz\right)|f''(z)|)}}{\int_0^{\frac{\pi}{2q}} \mathrm{d}z\sqrt{1 + f'^2(z)}}, \tag{21}$$

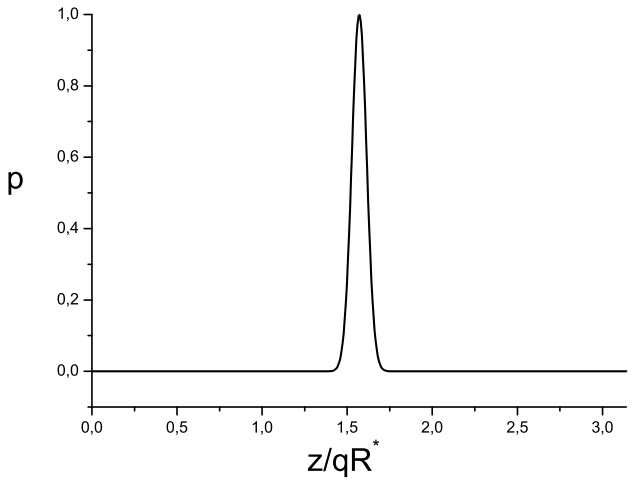

Fig. 5. Function $p(z)$, characterizing the asymmetry in the distribution of the side chains with respect to the backbone, as a function of position z along the bent section. A maximum in asymmetry takes place at the top of the bending.

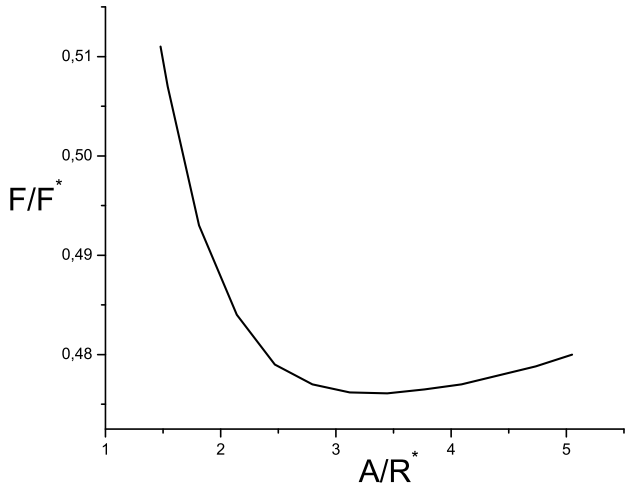

Fig. 6. Free energy as a function of the amplitude of bending after minimization with respect to the asymmetry parameter p. The function exhibits a minimum at $A \approx 3.3R^*$.

where $\sigma_-(z) = \sigma^*(1 - p(z))$. The total energy per side chain equals

$$F = \frac{1}{2\sigma^*}\left(F_+ + F_-\right).$$

An additional restriction relating parameters q and A follows from equation (20),

$$R^* = \frac{\pi}{2q}\frac{\sqrt{1+f'^2(0)}}{f'(0)} = \frac{\pi\sqrt{1+(Aq)^2}}{2Aq^2}. \qquad (22)$$

For minimization of the free energy we take the function $p(z)$ in the form $p(z) = B\sin^n(qz)$ where we put $B = 1$ thus avoiding singularity in the integral (Eq. (21)). Numerical calculations show that the minimum is attained at $n \approx 530$. The function $p(z)$ is plotted in Figure 5 and has a sharp maximum at the top of bending. It implies that the strongest redistribution of the side chains takes place at the point of maximum bending. The minimal free energy equals $F_{\min} \approx 0.476F^*$, $A \approx 3.3R^*$, $q \approx 1.6/R^*$, and the curvature at the top of bending is $C_{\max} \approx 8.5/R^*$. Thus, the bent brush has a deeper minimum and hence is more stable than the rectilinear brush. The plot of the free energy as a function of the amplitude of bending A is shown in Figure 6. From this picture we see that the free energy depends slightly on A for a broad range of values which means that the fluctuations in A can be large. Calculations show that at the same time the parameter q remains approximately constant.

4 Concluding remarks

In the present paper we addressed the bending of 2D copolymer brushes using the blob model. Our calculations differ from the mean-field approach based on the Alexander-de Gennes approximation used by Potemkin. The latter approximation implies that the local stability of the non-equilibrium rectilinear brush conformation with free ends all located at the same distance from the backbone was analyzed, rather than the equilibrium situation with free ends distributed throughout the layer. An analysis concerning the applicability of this approach was not given.

According to our calculations the rectilinear brush conformation is locally stable and spontaneous bending occuring without external action takes place only in the non-linear deformation regime when the curvature of bending exceeds some critical value, $C > C^* \sim 1/R^*$. The local stability is found both in a good solvent and in a solvent which is close to the θ-condition. This analysis, which is presented in the Appendices A and B, supports the use of a simple Daoud-Cotton blob picture for the investigation of the non-linear deformation regime, as this approach also predicts the correct local stability of the rectilinear brush. In addition, the analysis shows that the free energy of the rectilinear brush with relaxing free ends (see App. B) exceeds the corresponding free energy of the bent brush obtained from the general free-energy equation (B.3) in the scope of the Alexander-de Gennes approximation. Obviously, the last free energy corresponds to the non-equilibrium conformation and, therefore, overestimates the real minimal value.

Defining the persistence length of the rectilinear brush in the usual way we showed that it increases with increasing molecular weight of the side chains according to the scaling law $\lambda \sim M^3$. Based on the scaling approach we could distinguish two regimes which are separated by a potential barrier, namely a regime of stability against bending when $C < 1/R^*$ and a regime of spontaneous bending when $C > 1/R^*$. In the latter case the brush conformation is stabilized by the excluded-volume interactions between distant parts of the brush. We analyzed this situation in more detail and showed that the free energy of a side chain in the bent section of the brush is smaller than in a straight brush. Therefore bending is preferred. In the general case the global conformation of the brush

includes both rectilinear and bent sections. Of course, this picture should be supplemented by thermal fluctuations. Some indications for the presence of alternating rectilinear and bent sections, with an asymmetric distribution of side chains in the latter, have been obtained by Monte Carlo computer simulations of a 2D copolymer brush [19].

A. Subbotin acknowledges financial support from Netherlands Organization for Scientific Research (NWO) within the Dutch Russian scientific cooperation program. We thank A.N. Semenov for valuable comments.

Appendix A. Stability analysis of a rectilinear 2D brush: mean-field approach with relaxing free ends

In this appendix, we re-examine the results of reference [16] taking the distribution of the free ends into account. The free energy of a bent section with curvature C is the sum of the convex and concave part:

$$F = F_+(p) + F_-(p). \tag{A.1}$$

Here we use the same designations as in the main text, and the free energy is defined per unit length of the backbone. Denoting the concentration of the segments in the convex and concave parts as $\phi_+(x)$ and $\phi_-(x)$, and the thickness of the corresponding layers as R_+ and R_-, the free energies $F_+(p)$ and $F_-(p)$ are given by

$$\begin{aligned} F_+(p) &= \min_{\{\phi_+,R_+\}} F_+(\phi_+,R_+,\sigma_+),\\ F_-(p) &= \min_{\{\phi_-,R_-\}} F_-(\phi_-,R_-,\sigma_-). \end{aligned} \tag{A.2}$$

Let us first consider the free energy of the concave part. It consists of the elastic energy of the side chains and the interaction energy, which for marginal solvent can be written as [22–25]

$$\begin{aligned} F_- = \frac{1}{a^2}\int_0^{R_-} \mathrm{d}x_M(1-Cx_M)g_-(x_M)\int_0^{x_M}\mathrm{d}xE(x,x_M)\\ +v\int_0^{R_-}\mathrm{d}x(1-Cx)\phi_-^2(x), \end{aligned} \tag{A.3}$$

where a is the statistical segment length and v is the second virial coefficient. The distribution function of the free ends $g_-(x_M)$ is connected with the concentration by

$$\int_x^{R_-}\frac{\mathrm{d}x_M(1-Cx_M)g_-(x_M)}{E(x,x_M)} = (1-Cx)\phi_-(x), \tag{A.4}$$

where the function $E(x,x_M)$ characterizes the local chain stretching,

$$E(x,x_M) = \frac{\pi}{2M}\sqrt{x_M^2-x^2}\,. \tag{A.5}$$

Using equations (A.4, A.5) we find that

$$g_-(u) = -\frac{1}{M}\frac{1}{1-Cu}\frac{\mathrm{d}}{\mathrm{d}u}\left[\int_u^{R_-}\frac{\mathrm{d}x(1-Cx)x\phi_-(x)}{\sqrt{x^2-u^2}}\right]. \tag{A.6}$$

After substitution of this equation into (A.3) the free energy of the concave part is obtained:

$$\begin{aligned} F_- = \frac{\pi^2}{4M^2a^2}\int_0^{R_-}\mathrm{d}x(1-Cx)x^2\phi_-(x)\\ +v\int_0^{R_-}\mathrm{d}x(1-Cx)\phi_-^2(x). \end{aligned} \tag{A.7}$$

Minimization of the latter with respect to ϕ_- gives

$$\phi_-(x) = \phi_-^* - \frac{\pi^2x^2}{8M^2a^2v}\,. \tag{A.8}$$

The equilibrium thickness R_- of the layer follows from $\phi_-(R_-)=0$,

$$R_-^2 = \frac{8M^2a^2v\phi_-^*}{\pi^2}\,, \tag{A.9}$$

and ϕ_-^* is found from the normalization condition

$$\int_0^{R_-}\mathrm{d}x(1-Cx)\phi_-(x) = M\sigma_-. \tag{A.10}$$

Thus,

$$\begin{aligned} R_- &= R_-^*\left(1+\frac{1}{8}CR_-^* + \frac{3}{64}C^2R_-^{*2}\right),\\ R_-^* &= R^*\left(\frac{\sigma_-}{\sigma^*}\right)^{1/3} = R^*(1-p)^{1/3},\\ R^* &= aM\left(\frac{12v\sigma^*}{\pi^2a}\right)^{1/3} \end{aligned} \tag{A.11}$$

and the free energy of the concave layer is given by

$$\begin{aligned} F_-(p) = \frac{2aM}{5\pi v}\mu^{*5/2}\left((1-p)^{5/3} + \frac{5}{24}CR^*(1-p)^2\right.\\ \left.+\frac{5}{64}C^2R^{*2}(1-p)^{7/3}\right), \end{aligned} \tag{A.12}$$

where

$$\mu^* = \left(\frac{3\pi v\sigma^*}{2a}\right)^{1/3}. \tag{A.13}$$

Calculations for the convex layer are more complicated due to the appearance of the exclusion zone for the free ends near the backbone [22,26,27]. Assuming that for $0 \le x_M \le r$, $g_+(u)=0$, and for $r \le x_M \le R_+$, $g_+(u) \ge 0$, the free energy is given by

$$\begin{aligned} F_+ = \frac{1}{a^2}\int_r^{R_+}\mathrm{d}x_M(1+Cx_M)g_+(x_M)\int_0^{x_M}\mathrm{d}xE(x,x_M)\\ +v\int_0^{R_+}\mathrm{d}x(1+Cx)\phi_+^2(x). \end{aligned} \tag{A.14}$$

The function $E(x, x_M)$ can be expressed through the chemical potential $\mu(x) = 2v\phi_+(x)$ as

$$E(x, x_M) = a\sqrt{\mu(x) - \mu(x_M)}. \tag{A.15}$$

The equation connecting the free-ends distribution function and the concentration is given by

$$\int_x^{R_+} \frac{\mathrm{d}x_M(1 + Cx_M)g_+(x_M)}{a\sqrt{\mu(x) - \mu(x_M)}} = (1 + Cx)\phi_+(x). \tag{A.16}$$

From this we find ($\phi_+(x) = \mu(x)/(2v)$)

$$g_+(u) = \frac{a}{2v\pi}\frac{1}{1 + Cu}\frac{\mathrm{d}}{\mathrm{d}u}\left[\int_u^{R_+} \frac{\mathrm{d}x(1 + Cx)\mu(x)}{\sqrt{\mu(u) - \mu(x)}}\frac{\mathrm{d}\mu(x)}{\mathrm{d}x}\right] \tag{A.17}$$

and the normalization condition is

$$\int_r^{R_+} dx(1 + Cx)g_+(x) = \sigma_+. \tag{A.18}$$

Using equation (A.17) we get an equation for the function $\frac{\mathrm{d}x}{\mathrm{d}\mu}$,

$$C\int_0^{\mu} \mathrm{d}\mu' \frac{\mathrm{d}x}{\mathrm{d}\mu'}\frac{2\mu - \mu'}{\sqrt{\mu - \mu'}} = -2\sqrt{\mu}\,(1 + CR_+)\,. \tag{A.19}$$

Here $\mu_r = \mu(r) < \mu < \mu_0 = \mu(0)$. The chain length M and the function $\frac{\mathrm{d}x}{\mathrm{d}\mu}$ are connected by means of the equation

$$\int_{\mu}^{\mu_0} \frac{\mathrm{d}x}{\mathrm{d}\mu'}\frac{\mathrm{d}\mu'}{\sqrt{\mu' - \mu}} = -aM. \tag{A.20}$$

Next we introduce a new function $m(\mu)$ as

$$m(\mu) = -\frac{1}{a}\int_{\mu}^{\mu_0} \frac{\mathrm{d}x}{\mathrm{d}\mu'}\frac{\mathrm{d}\mu'}{\sqrt{\mu' - \mu}}, \quad \mu_r \le \mu \le \mu_0\,, \tag{A.21}$$
$$m(\mu) = M, \qquad \mu(R_+) = 0 \le \mu \le \mu_r$$

and express the derivative $\frac{\mathrm{d}x}{\mathrm{d}\mu}$ through $\frac{\mathrm{d}m}{\mathrm{d}\mu}$ using equation (A.20),

$$\frac{\mathrm{d}x}{\mathrm{d}\mu} = \frac{a}{\pi}\int_{\mu}^{\mu_0} \frac{\mathrm{d}m}{\mathrm{d}\mu'}\frac{\mathrm{d}\mu'}{\sqrt{\mu' - \mu}}, \quad \mu_r < \mu < \mu_0\,, \tag{A.22}$$

$$\frac{\mathrm{d}x}{\mathrm{d}\mu} = \frac{a}{\pi}\int_{\mu_r}^{\mu_0} \frac{\mathrm{d}m}{\mathrm{d}\mu'}\frac{\mathrm{d}\mu'}{\sqrt{\mu' - \mu}}, \quad 0 < \mu < \mu_r\,. \tag{A.23}$$

Substitution of the last equations in (A.19) gives an equation for $\frac{\mathrm{d}m}{\mathrm{d}\mu}$ (see [27])

$$\int_{\mu_r}^{\mu_0} \mathrm{d}\mu' \frac{\mathrm{d}m}{\mathrm{d}\mu'}\left[\frac{1}{2}\left(3 - \frac{\mu'}{\mu}\right)\ln\frac{\sqrt{\mu} + \sqrt{\mu'}}{\mid\sqrt{\mu} - \sqrt{\mu'}\mid} + \sqrt{\frac{\mu'}{\mu}}\right] = -\frac{2\pi}{aC}\frac{(1 + CR_+)}{\sqrt{\mu}}. \tag{A.24}$$

Taking into account that $aMC \ll 1$ and $\mu_0 - \mu_r \ll \mu_0$, the last integral equation can in a first approximation be written as Carleman's equation,

$$\int_{\mu_r}^{\mu_0} \mathrm{d}\mu' \frac{\mathrm{d}m}{\mathrm{d}\mu'}\ln\frac{\mid\mu - \mu'\mid}{4\mu_0} = \frac{2\pi}{aC}\frac{1}{\sqrt{\mu}} \tag{A.25}$$

which has the following solution [28,29] (we omit small terms of order $\mu_0 - \mu_r$):

$$\frac{\mathrm{d}m}{\mathrm{d}\mu} = \frac{2}{aC\sqrt{\mu_0}\ln\left[\frac{1}{16\mu_0}(\mu_0 - \mu_r)\right]}\frac{1}{\sqrt{\mu_0 - \mu}\sqrt{\mu - \mu_r}} = -\frac{M}{\pi\sqrt{\mu_0 - \mu}\sqrt{\mu - \mu_r}}\,. \tag{A.26}$$

In the last equality we used the fact that $m(\mu_r) = M$. From equation (A.26) we find that the difference between the chemical potentials at the boundaries of the exclusion zone is exponentially small (see also [26]),

$$\mu_0 - \mu_r = 16\mu_0 e^{-\frac{2\pi}{aMC\sqrt{\mu_0}}}. \tag{A.27}$$

Similarly, the exclusion zone thickness is also exponentially small,

$$r = 4aM\sqrt{\mu_0 - \mu_r} = 16aM\sqrt{\mu_0}e^{-\frac{\pi}{aMC\sqrt{\mu_0}}}. \tag{A.28}$$

After some calculations the free energy can be written as

$$F_+ = \frac{2aM}{5\pi v}\mu_r^{5/2}(1 - CR_+) + \frac{3\sigma_+}{2a}\int_0^r \mathrm{d}x\sqrt{\mu(x) - \mu(r)} + \frac{aMC}{4\pi v}\int_r^{R_+} \mathrm{d}x\left[\frac{2}{5}\left(\mu(r) - \mu(x)\right)^{5/2} - 2\mu_r^2\sqrt{\mu(r) - \mu(x)}\right]. \tag{A.29}$$

Using equations (A.22, A.23, A.26) and the normalization condition for the concentration $\phi_+(x) = \mu(x)/(2v)$,

$$\int_0^{R_+} \mathrm{d}x(1 + Cx)\mu(x) = 2Mv\sigma_+\,, \tag{A.30}$$

we get the final expression for the free energy of the convex part,

$$F_+(p) = \frac{2aM}{5\pi v}\mu^{*5/2}\left((1 + p)^{5/3} - \frac{5}{24}CR^*(1 + p)^2 + \frac{5}{64}C^2R^{*2}(1 + p)^{7/3}\right). \tag{A.31}$$

Note, the exclusion zone is not essential in this case. Minimization of the total energy $F = F_+(p) + F_-(p)$ with respect to p shows that the quadratic term in the expansion of the free energy as a function of C is zero, *i.e.* $\lambda = 0$. It implies that for the stability analysis the third virial coefficient should be taken into account.

Based on the above approach and expanding the interaction energy up to the third virial coefficient, the total free energy of the concave part is given by

$$F_- = \frac{\pi^2}{4M^2a^2}\int_0^{R_-} \mathrm{d}x x^2\phi_-(x) + \int_0^{R_-} \mathrm{d}x(1-Cx)\left(v\phi_-^2(x)+w\phi_-^3(x)\right). \quad \text{(A.32)}$$

Minimization of the last energy with respect to ϕ_- gives

$$\phi_-(x) = \frac{v}{3w}\left[\sqrt{1+\frac{6w\phi_-^*}{v}\left(1-\frac{\pi^2x^2}{8M^2a^2v\phi_-^*}\right)}-1\right], \quad \text{(A.33)}$$

where ϕ_-^* is found from the normalization condition, equation (A.10), using an expansion in the small parameter $\frac{w\phi_-^*}{v}$. The equilibrium thickness R_- of the layer follows from the equation $\phi_-(R_-)=0$,

$$R_- = R_-^*\left(1+\frac{1}{8}CR_-^*+\frac{3}{64}C^2R_-^{*2} + \frac{\pi^2wR_-^{*2}}{20v^2a^2M^2}\left(1+\frac{9}{16}CR_-^*+\frac{3}{8}C^2R_-^{*2}\right)\right), \quad \text{(A.34)}$$

$$R_-^* = aM\left(\frac{12v\sigma_-}{\pi^2a}\right)^{1/3}.$$

Further, following the same procedure as before we find that the free energy of the concave layer is given by

$$F_-(p) = \frac{2aM}{5\pi v}\mu^{*5/2}\left[(1-p)^{5/3}+\frac{2\epsilon}{7}(1-p)^{7/3} + \frac{5}{24}CR^*\left((1-p)^2+\frac{33\epsilon}{40}(1-p)^{8/3}\right) + \frac{5}{64}C^2R^{*2}\left((1-p)^{7/3}+\frac{13\epsilon}{5}(1-p)^3\right)\right], \quad \text{(A.35)}$$

where

$$\epsilon = \frac{w\mu^*}{v^2} \ll 1. \quad \text{(A.36)}$$

Similarly, the free energy of the convex layer is

$$F_+(p) = \frac{2aM}{5\pi v}\mu^{*5/2}\left((1+p)^{5/3}+\frac{2\epsilon}{7}(1+p)^{7/3} - \frac{5}{24}CR^*\left((1+p)^2+\frac{33\epsilon}{40}(1+p)^{8/3}\right) + \frac{5}{64}C^2R^{*2}\left((1+p)^{7/3}+\frac{13\epsilon}{5}(1+p)^3\right)\right]. \quad \text{(A.37)}$$

Minimization of the total energy $F=F_+(p)+F_-(p)$ with respect to p gives the following quadratic term in the expansion of the free energy as a function of C:

$$\Delta F = \frac{w}{10}\left(\frac{aM}{\pi v}\right)^3\mu^{*9/2}C^2. \quad \text{(A.38)}$$

The sign of the front factor is positive implying local stability of the rectilinear brush. The persistence length equals

$$\lambda = \frac{w}{5}\left(\frac{aM}{\pi v}\right)^3\mu^{*9/2}\sim M^3. \quad \text{(A.39)}$$

Appendix B. Stability analysis of the swollen rectilinear 2D brush with relaxing free ends

In this appendix, we consider the stability of the 2D rectilinear brush with relaxing free ends in a good solvent. As before, the free energy of a bent section with curvature-C brush includes the convex and concave part,

$$F = F_+(\sigma_+)+F_-(\sigma_-), \quad \text{(B.1)}$$

where the free energies $F_+(\sigma_+)$ and $F_-(\sigma_-)$ are given by

$$F_+(\sigma_+) = \min_{\{\phi_+,R_+\}} F_+(\phi_+,R_+,\sigma_+), \qquad F_-(\sigma_-) = \min_{\{\phi_-,R_-\}} F_-(\phi_-,R_-,\sigma_-). \quad \text{(B.2)}$$

Here $\phi_+(x)$, $\phi_-(x)$ are the volume fractions of the side chain segments, and R_+, R_- is the thickness of the convex and concave layer, respectively. We start with the free energy of the concave layer which, per unit length of the backbone, can be written as (see [23])

$$F_- = \frac{1}{a^2}\int_0^{R_-}\mathrm{d}x_M(1-Cx_M)g_-(x_M) \times\int_0^{x_M}\mathrm{d}xE(x,x_M)\phi_-^\alpha(x) + \frac{1}{a^d}\int_0^{R_-}\mathrm{d}x(1-Cx)\phi_-^\beta(x), \quad \text{(B.3)}$$

where a is the segment length (it is assumed that the segment volume equals a^d), dimension $d=2$, $\nu=3/4$, $\alpha=(2\nu-1)/(d\nu-1)=1$, $\beta=\mathrm{d}\nu/(\mathrm{d}\nu-1)=3$, and $E(x,x_M)=\frac{\mathrm{d}x}{\mathrm{d}n}$ is the local chain stretching. The distribution function of the free ends $g_-(x_M)$ is connected with the concentration by

$$\int_x^{R_-}\frac{\mathrm{d}x_M(1-Cx_M)g_-(x_M)a^2}{E(x,x_M)} = (1-Cx)\phi_-(x) \quad \text{(B.4)}$$

and the chain length M is connected with the function $E(x,x_M)$ by

$$M = \int_0^{x_M}\frac{\mathrm{d}x}{E(x,x_M)}. \quad \text{(B.5)}$$

Minimization of the free energy (B.3), with the additional equations (B.4, B.5), with respect to $E(x,x_M)$ gives

$$E(x,x_M) = a\phi_-^{\alpha/2}(x)\sqrt{\mu(x)-\mu(x_M)}, \quad \text{(B.6)}$$

where

$$\mu(x) = \mu(0)-\frac{\pi^2}{4M^2a^2}\left(\int_0^x\mathrm{d}x'\phi_-^{\alpha/2}(x')\right)^2. \quad \text{(B.7)}$$

Using equations (B.4, B.6) we find that

$$g_-(u) = \frac{1}{\pi a}\frac{1}{1-Cu}\frac{\mathrm{d}}{\mathrm{d}u}\left[\int_u^{R_-}\frac{\mathrm{d}x(1-Cx)\phi_-^{1-\alpha/2}(x)}{\sqrt{\mu(u)-\mu(x)}}\frac{\mathrm{d}\mu(x)}{\mathrm{d}x}\right]. \quad \text{(B.8)}$$

After substitution of this equation into equation (B.3) the free energy of the concave part is obtained

$$F_- = \frac{\pi^2}{4M^2a^4}\int_0^{R_-}\mathrm{d}x(1-Cx)\left(\int_0^x \mathrm{d}x'\phi_-^{\alpha/2}(x')\right)^2\phi_-(x) + \frac{1}{a^2}\int_0^{R_-}\mathrm{d}x(1-Cx)\phi_-^{\beta}(x). \quad \text{(B.9)}$$

Let us introduce a new variable,

$$y = \int_0^x \mathrm{d}x'\phi_-^{\alpha/2}(x'), \qquad y_- = \int_0^{R_-}\mathrm{d}x'\phi_-^{\alpha/2}(x') \quad \text{(B.10)}$$

and rewrite the free energy (B.9) in the form ($\psi_-(y) = \phi_-(x)$)

$$F_- = \frac{\pi^2}{4M^2a^4}\int_0^{y_-}\mathrm{d}y(1-Cx(y))y^2\psi_-^{1-\alpha/2}(y) + \frac{1}{a^2}\int_0^{y_-}\mathrm{d}y(1-Cx(y))\psi_-^{\beta-\alpha/2}(y). \quad \text{(B.11)}$$

Minimization of the last energy with respect to ψ_- using the normalization condition

$$\int_0^{y_-}\mathrm{d}y(1-Cx(y))\psi_-^{1-\alpha/2}(y) = Ma^2\sigma_- \quad \text{(B.12)}$$

gives

$$\psi_-(y) = \left[\frac{\pi^2}{4a^2M^2}\frac{1-\alpha/2}{\beta-\alpha/2}\right]^{\frac{1}{\beta-1}}\left(y_-^2-y^2\right)^{\frac{1}{\beta-1}}. \quad \text{(B.13)}$$

Substitution of the last function into the normalization equation (B.12) results in the equation for y_-,

$$Ma^2\sigma_- = I_1\left[\frac{\pi^2}{4a^2M^2}\frac{1-\alpha/2}{\beta-\alpha/2}\right]^{\frac{1-\alpha/2}{\beta-1}}y_-^{\frac{\beta-\alpha+1}{\beta-1}} - CI_2\left[\frac{\pi^2}{4a^2M^2}\frac{1-\alpha/2}{\beta-\alpha/2}\right]^{\frac{1-\alpha}{\beta-1}}y_-^{\frac{2(\beta-\alpha)}{\beta-1}}, \quad \text{(B.14)}$$

where

$$I_1 = \int_0^{\pi/2}\mathrm{d}\varphi\cos^{\frac{\beta-\alpha+1}{\beta-1}}(\varphi) \approx 0.874,$$

$$I_2 = \int_0^{\pi/2}\mathrm{d}\varphi\cos^{\frac{\beta-\alpha+1}{\beta-1}}(\varphi)\int_0^{\varphi}\mathrm{d}\varphi'\cos^{\frac{\beta-\alpha-1}{\beta-1}}(\varphi') \approx 0.421.$$

From this we find

$$y_- = y_-^*\left(1+\frac{2}{3}\frac{I_2}{I_1}aMC\left(\frac{20a\sigma_-}{\pi^2I_1}\right)^{1/3} + \frac{7}{9}\left(\frac{I_2}{I_1}aMC\right)^2\left(\frac{20a\sigma_-}{\pi^2I_1}\right)^{2/3}\right), \qquad y_-^* = Ma\left(\frac{a\sigma_-}{I_1}\right)^{2/3}\left(\frac{20}{\pi^2}\right)^{1/6}. \quad \text{(B.15)}$$

Using equations (B.13, B.14) the free energy (B.11) can be written as

$$F_-(y_-,\sigma_-) = \frac{3\pi^2y_-^2\sigma_-}{28a^2M} - \frac{\pi^2y_-^4C}{70a^4M^2}. \quad \text{(B.16)}$$

Substitution of y_- from equation (B.15) gives the final expression for the free energy of the concave layer,

$$F_-(\sigma_-) \approx 1.601\frac{M}{a}\left((a\sigma_-)^{7/3} + 0.649aMC(a\sigma_-)^{8/3} + 0.976(aMC)^2(a\sigma_-)^3\right). \quad \text{(B.17)}$$

The free energy of the convex part without the exclusion zone for the free ends can be obtained by replacing $C \to -C$ in equation (B.17),

$$F_+(\sigma_+) \approx 1.601\frac{M}{a}\left((a\sigma_+)^{7/3} - 0.649aMC(a\sigma_+)^{8/3} + 0.976(aMC)^2(a\sigma_+)^3\right). \quad \text{(B.18)}$$

Thus, after minimization of the total energy $F = F_+(\sigma_+) + F_-(\sigma_-) = F_+(\sigma^*(1+p)) + F_-(\sigma^*(1-p))$ with respect to p, the quadratic term in the expansion of the total energy is given by

$$\Delta F \approx 1.583a(Ma\sigma^*)^3C^2. \quad \text{(B.19)}$$

The rectilinear brush is again stable against small bending and the persistence length equals

$$\lambda \approx 3.167a(Ma\sigma^*)^3 \sim M^3. \quad \text{(B.20)}$$

References

1. T. Birshtein, O. Borisov, E. Zhulina, A. Khokhlov, T. Yurasova, Polymer Sci. USSR **29**, 1293 (1987).
2. G. Fredrickson, Macromolecules **26**, 2825 (1993).
3. A. Subbotin, M. Saariaho, O. Ikkala, G. ten Brinke, Macromolecules **33**, 3447 (2000).
4. R. Stepanyan, A. Subbotin, G. ten Brinke, Macromolecules **35**, 5640 (2002).
5. L. Feuz, F.A.M. Leermakers, M. Textor, O. Borisov, Macromolecules **38**, 8891 (2005).
6. M. Wintermantel, M. Gerle, K. Fischer, M. Schmidt, I. Wataoka, H. Urakawa, K. Kajiwara, Y. Tsukahara, Macromolecules **29**, 978 (1996).
7. S. Sheiko, M. Möller, Chem. Rev. **101**, 4099 (2001).
8. S. Lecommandoux, F. Chécot, R. Borsali, M. Schappacher, A. Deffieux, A. Brûlet, J.P. Cotton, Macromolecules **35**, 8878 (2002).
9. T. Stephan, S. Muth, M. Schmidt, Macromolecules **35**, 9857 (2002).
10. Y. Rouault, O.V. Borisov, Macromolecules **29**, 2605 (1996).
11. M. Saariaho, O. Ikkala, I. Szleifer, I. Erukhimovich, G. ten Brinke, J. Chem. Phys. **107**, 3267 (1997).
12. M. Saariaho, I. Szleifer, O. Ikkala, G. ten Brinke, Macromol. Theory Simul. **7**, 211 (1998).

13. R. Connolly, G. Bellesia, E.G. Timoshenko, Y.A. Kuznetsov, S. Elli, F. Ganazzoli, Macromolecules **38**, 5288 (2005).
14. J. de Jong, G. ten Brinke, Macromol. Theory Simul. **13**, 318 (2004).
15. P.G. Khalatur, A.R. Khokhlov, S.A. Prokhorova, S.S. Sheiko, M. Möller, P. Reineker, D.G. Shirvanyanz, N. Starovoitova, Eur. Phys. J. E **1**, 99 (2000).
16. I. Potemkin, Eur. Phys. J. E **12**, 207 (2003).
17. I. Potemkin, A. Khokhlov, S. Prokhorova, S. Sheiko, M. Möller, K. Beers, K. Matyjaszewski, Macromolecules **37**, 3918 (2004).
18. M.O. Gallyamov, B. Tartsch, A.R. Khokhlov, S.S. Sheiko, H.G. Börner, K. Matyjaszewski, M. Möller, Macromol. Rapid Commun. **25**, 1703 (2004).
19. J. de Jong, A. Subbotin, G. ten Brinke, Macromolecules **38**, 6718 (2005).
20. M. Daoud, J. Cotton, J. Phys. (Paris) **43**, 531 (1982).
21. T.M. Birshtein, E.B. Zhulina, Macromol. Theory Simul. **6**, 1169 (1997).
22. A.N. Semenov, Sov. Phys. JETP **61**, 733 (1985).
23. S.T. Milner, T.A. Witten, M.E. Cates, Macromolecules **21**, 2610 (1988).
24. E.B. Zhulina, O.V. Borisov, V.A. Priamitsin, J. Colloid Interface Sci. **137**, 495 (1989).
25. A.E. Likhtman, A.N. Semenov, Macromolecules **27**, 3103 (1994).
26. R.S. Ball, J.F. Marco, S.T. Milner, T.A. Witten, Macromolecules **24**, 693 (1991).
27. H. Li, T.A. Witten, Macromolecules **27**, 449 (1994).
28. F.D. Gakhov, *Boundary Value Problems* (in Russian, Nauka, Moscow, 1977).
29. A.D. Polyanin, A.V. Manzhirov, *Handbook of Integral Equations* (CRC Press, Boca Raton, 1998).